7.1.4 Photolithography

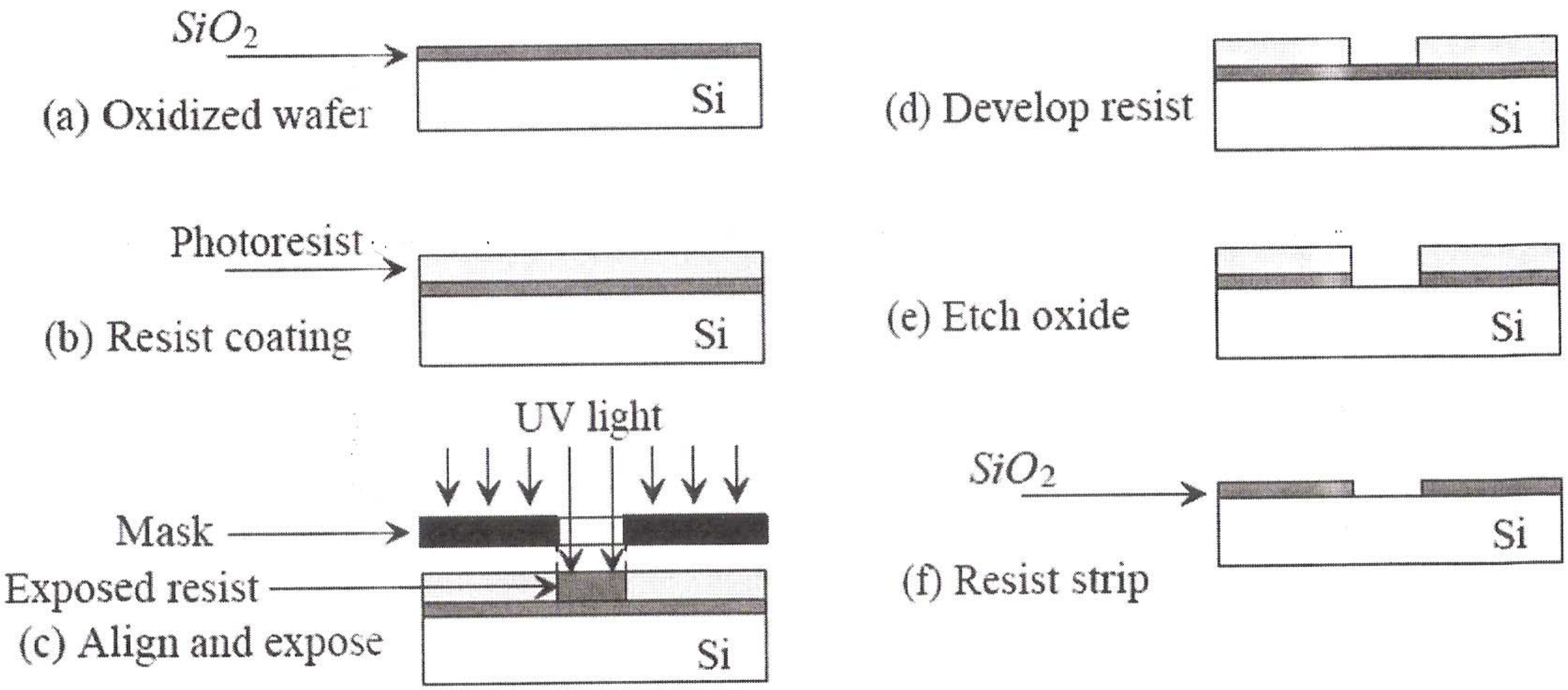

Figure 7.8 Simplified representation of the primary steps required for the implementation of photolighography and pattern transfer.

Figures from CMOS Circuit Design, Layout, and Simulation, Copyright Wiley-IEEE, CMOSedu.com

1)

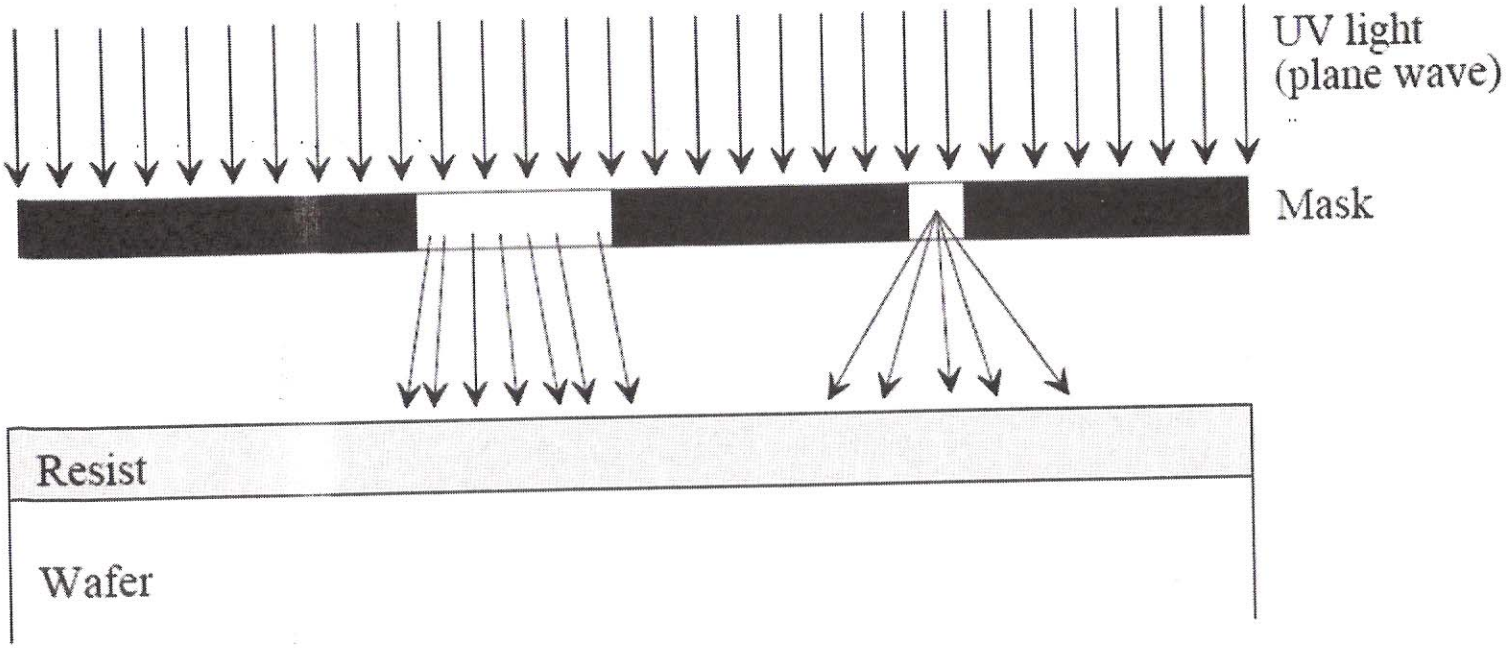

Figure 7.9 The diffraction effects become significant as the mask feature dimensions approach the wavelength of UV light. Notice that the diffraction angle is larger for the smaller opening.

Resolution → resolution, depth of

↑ critical parameters associated with a projection stepper

constant

wavelength

Minimum feature size, $M = \frac{C_1 \lambda}{NA}$

$NA \leftarrow N \cdot \sin\theta$

2)

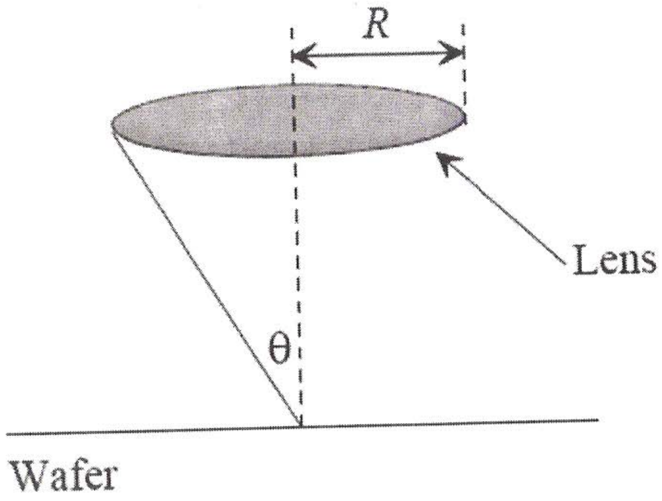

Figure 7.10 The relationship of the lens radii to the angle used to compute NA.

$NA = N \cdot \sin\theta$

numerical Aperture

index of refraction between space & lens.

3)

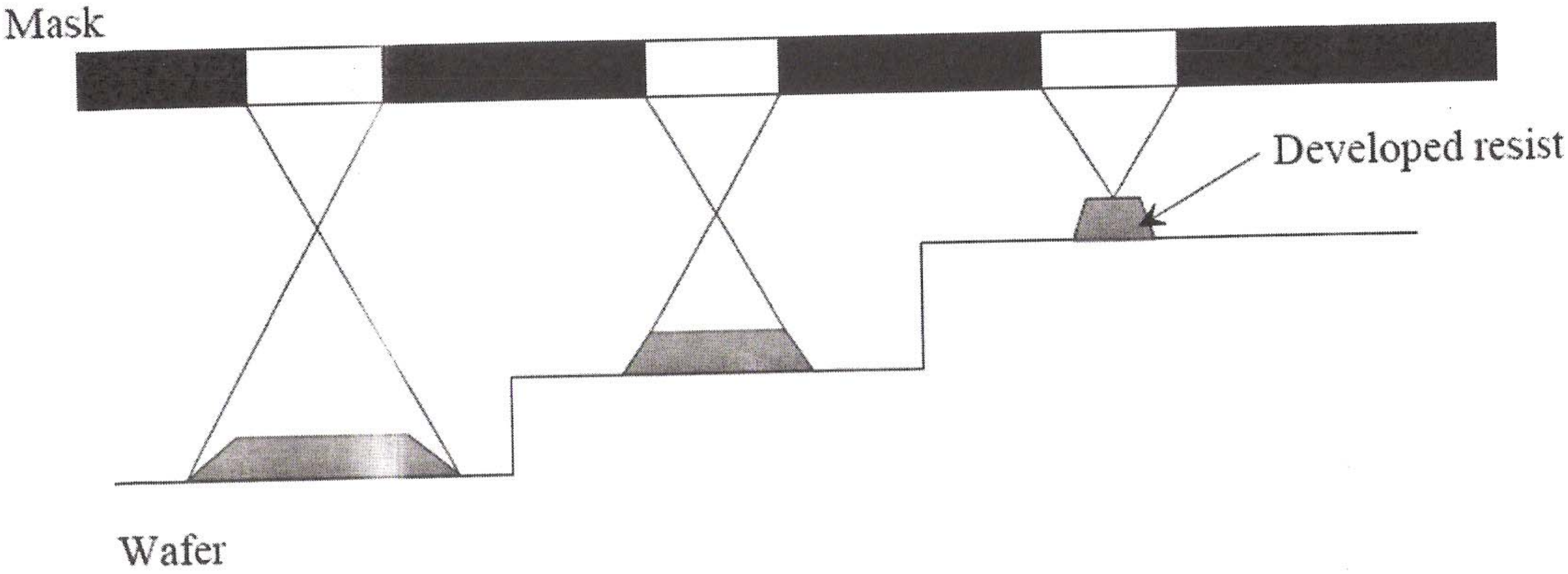

Figure 7.11 Depth of focus diagram illustrating the need to have planar surfaces (minimized topography) during high resolution photopatterning.

Depth of Focus (DDF) $= \frac{C_2 \lambda}{NA^2}$

$0.5 < C_2 < 1$

Figures from CMOS Circuit Design, Layout, and Simulation, Copyright Wiley-IEEE, CMOSedu.com

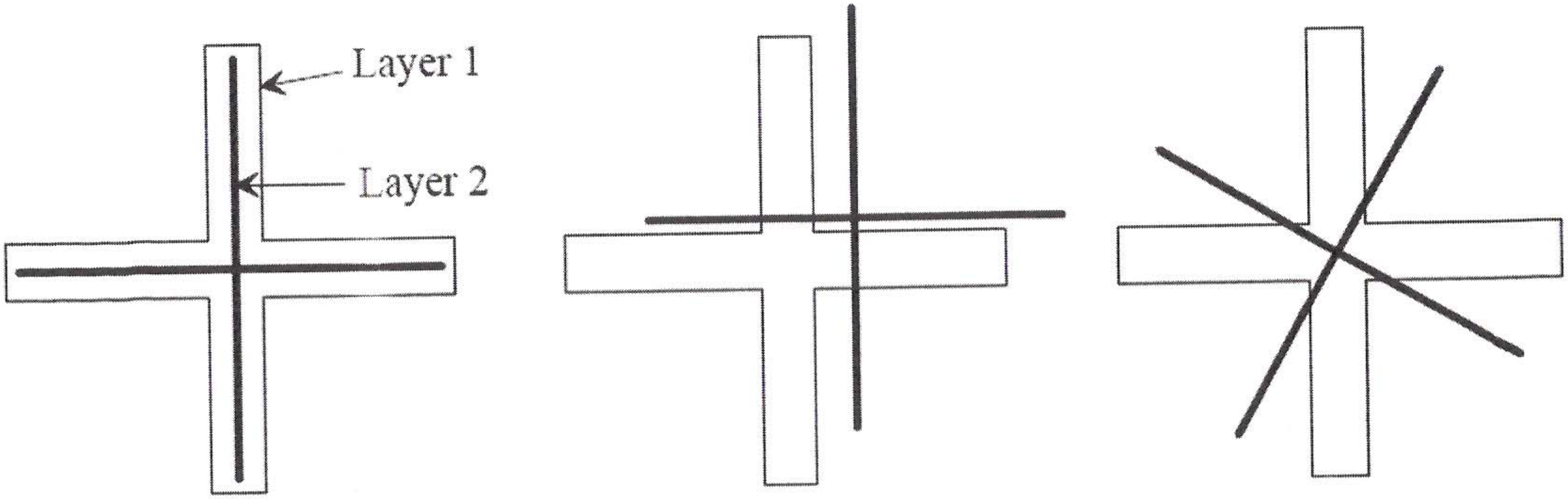

(a) No registration error

(b) x-y registration error

(c) z-rotation registration error.

Figure 7.12 Simple registration errors that can occur during wafer-to-mask alignment in photolithography. Other registration errors exist but are not discussed here.

5)

Figures from CMOS Circuit Design, Layout, and Simulation, Copyright Wiley-IEEE, CMOSedu.com

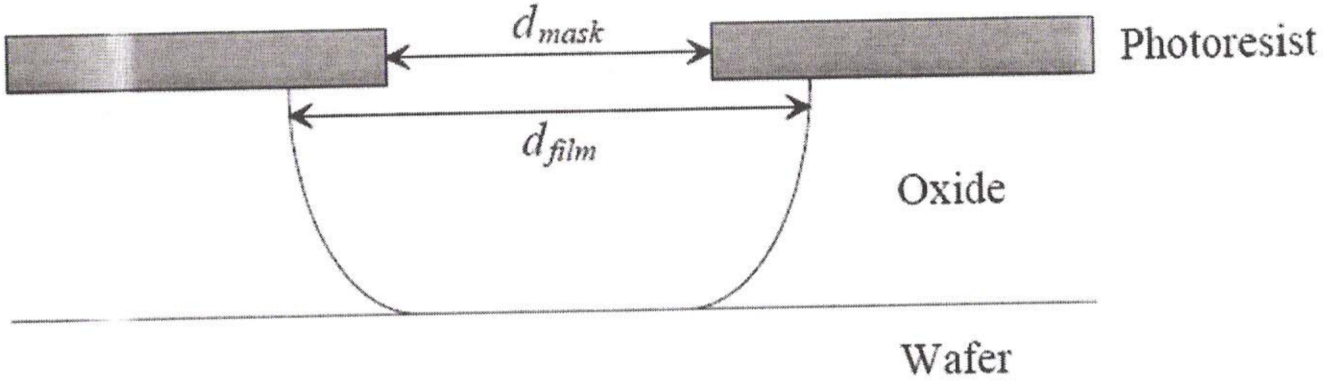

Figure 7.13 Diagram showing a post-etch profile. Notice that because of isotropy in the etch process the mask opening does not match the fabricated opening in the underlying oxide film. The difference between these dimensions is called etch-bias.

$$S = \frac{R_2}{R_1}$$

$$A_f = 1 - \frac{R_\ell}{R_v}$$

isotropic etch $A_f = 0$

$A_f = 1$, $R_\ell = 0$, $R_v = 1$

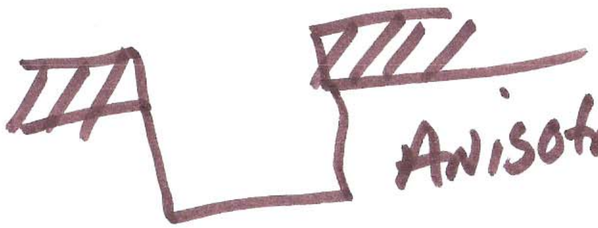

Anisotropic

6)

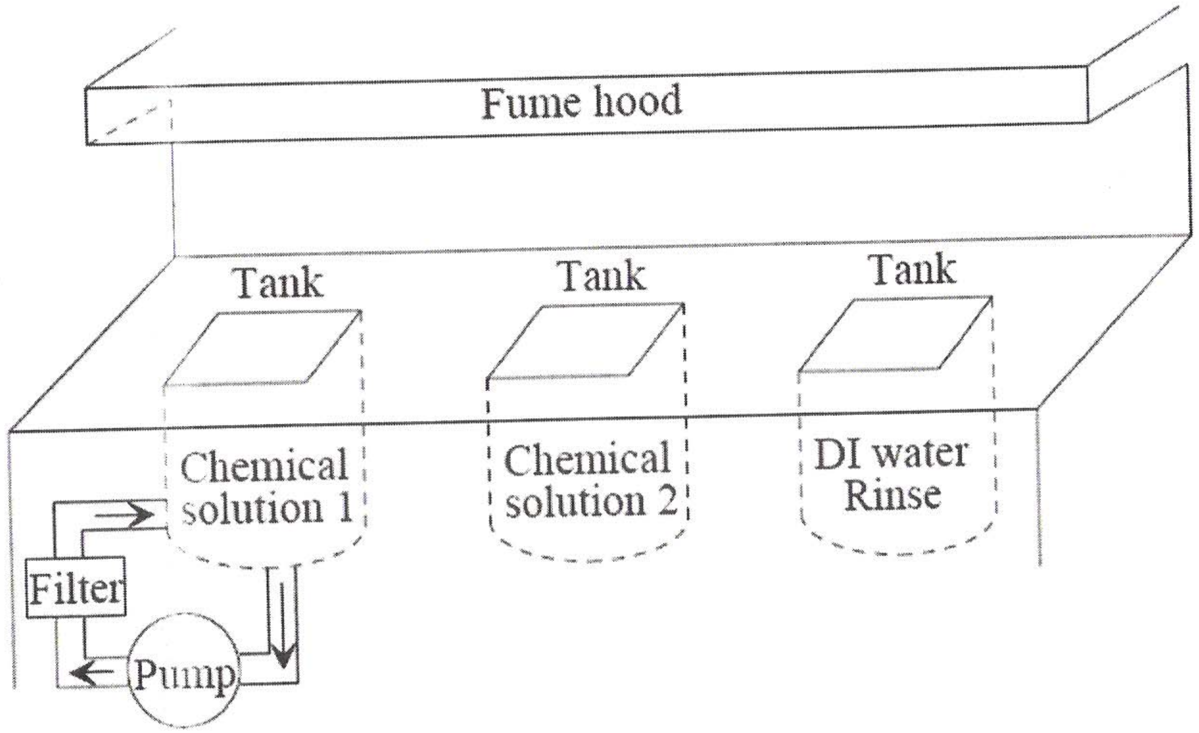

Figure 7.14 Simplfied diagram of a wet bench used for wet chemical cleaning and etching.

7)

Figures from CMOS Circuit Design, Layout, and Simulation, Copyright Wiley-IEEE, CMOSedu.com

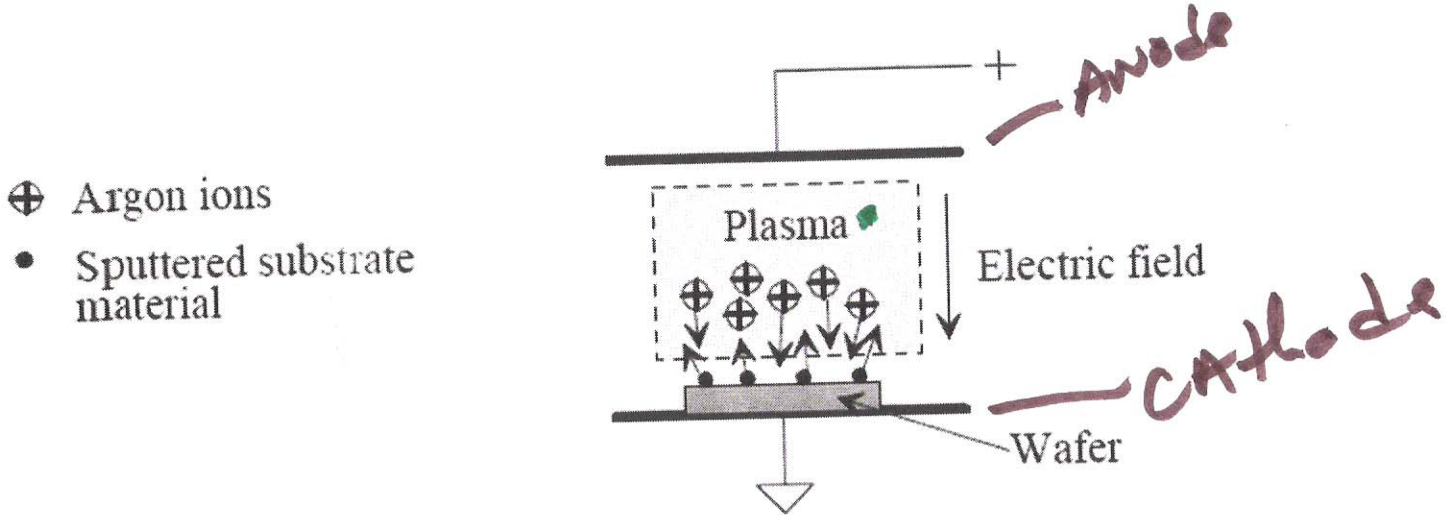

Figure 7.15 Simplified schematic diagram of the sputter etch process. This process is dominated by the physical bombardment of ions on a substrate.

Dry etch techniques:

- Sputter etching
- plasma etching
- reactive ion etching (RIE)

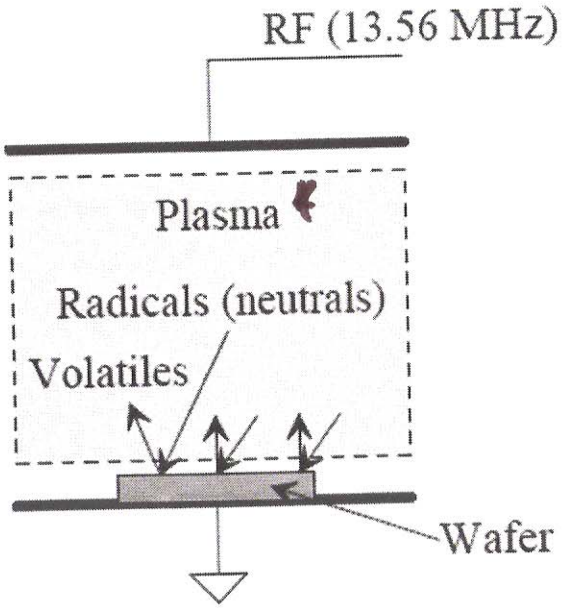

Figure 7.16 Simplified schematic diagram of a plasma etch process. This process is dominated by the chemical reactions of radicals at the surface of the substrate.

9)

Figures from CMOS Circuit Design, Layout, and Simulation, Copyright Wiley-IEEE, CMOSedu.com

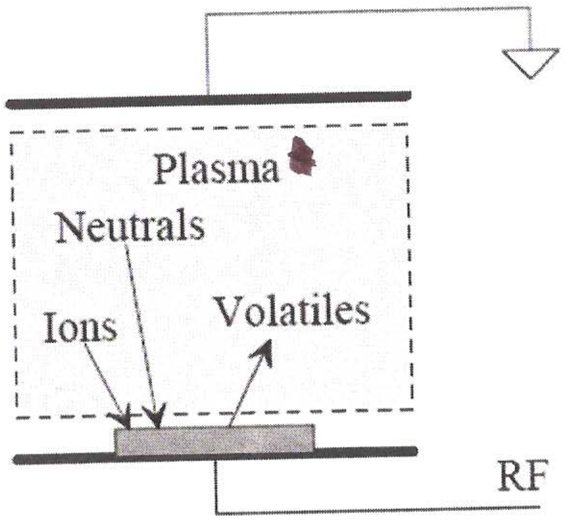

Figure 7.17 Simplified schematic diagram of an RIE etch process. This process has both physical (ion bombardment) and chemical (reaction of radicals) components.

10)

Figures from CMOS Circuit Design, Layout, and Simulation, Copyright Wiley-IEEE, CMOSedu.com

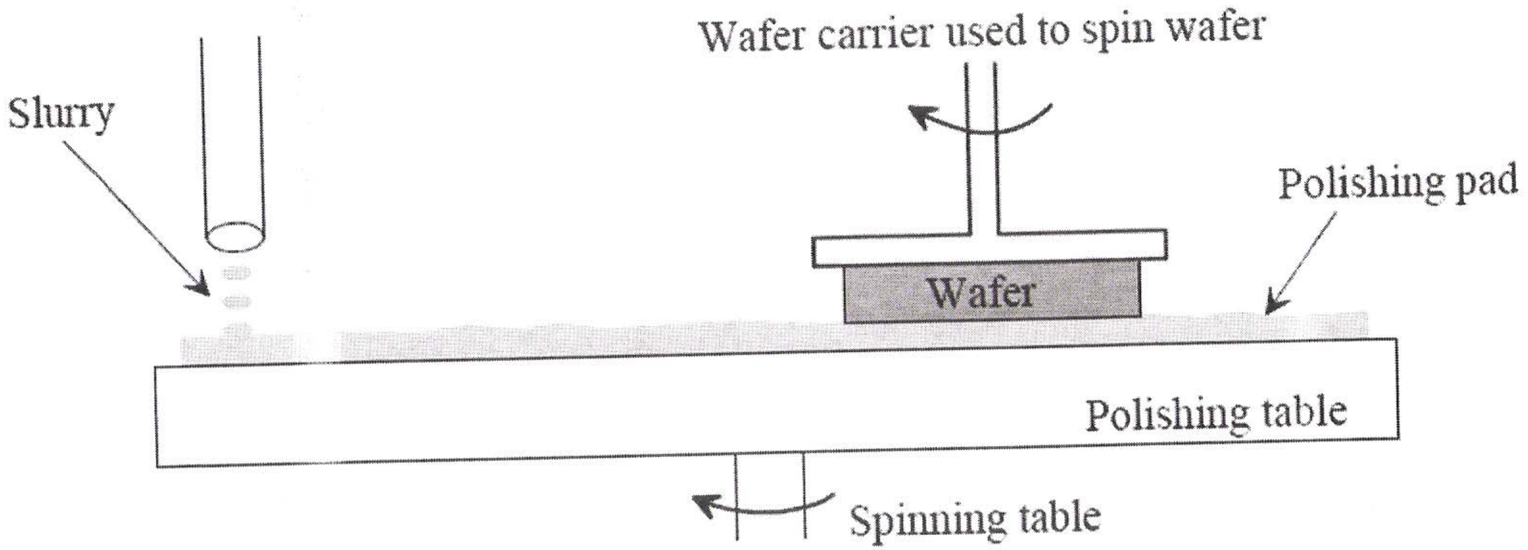

Figure 7.18 Simplified representation of a chemical mechanical polishing process used in the fabrication process.

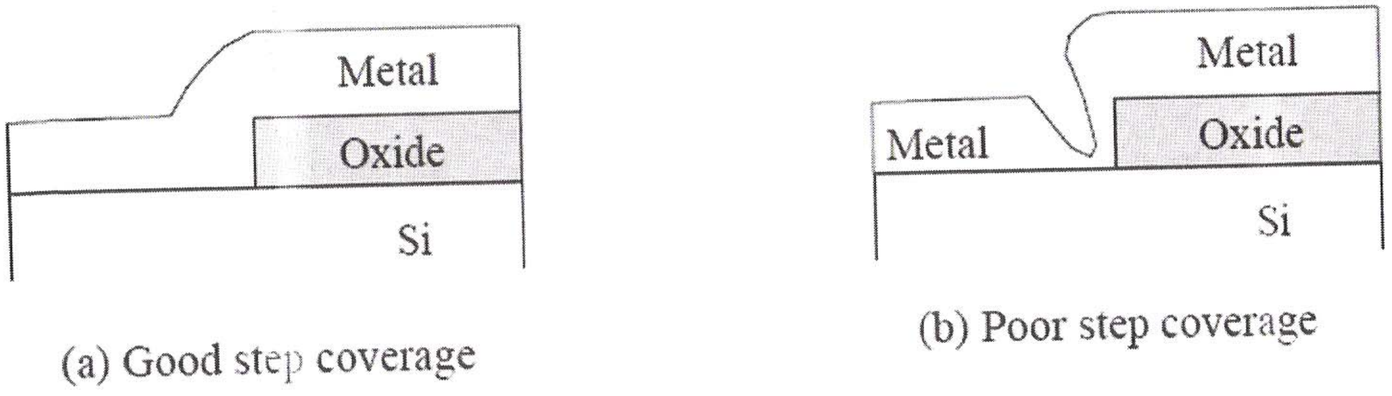

(a) Good step coverage

(b) Poor step coverage

Figure 7.19 Extremes in thin-film deposition coverage over a pre-existing oxide step.

PVD - Physical VApor Depositi..

CVD - CHemical VApor "

12)

Figures from CMOS Circuit Design, Layout, and Simulation, Copyright Wiley-IEEE, CMOSedu.com

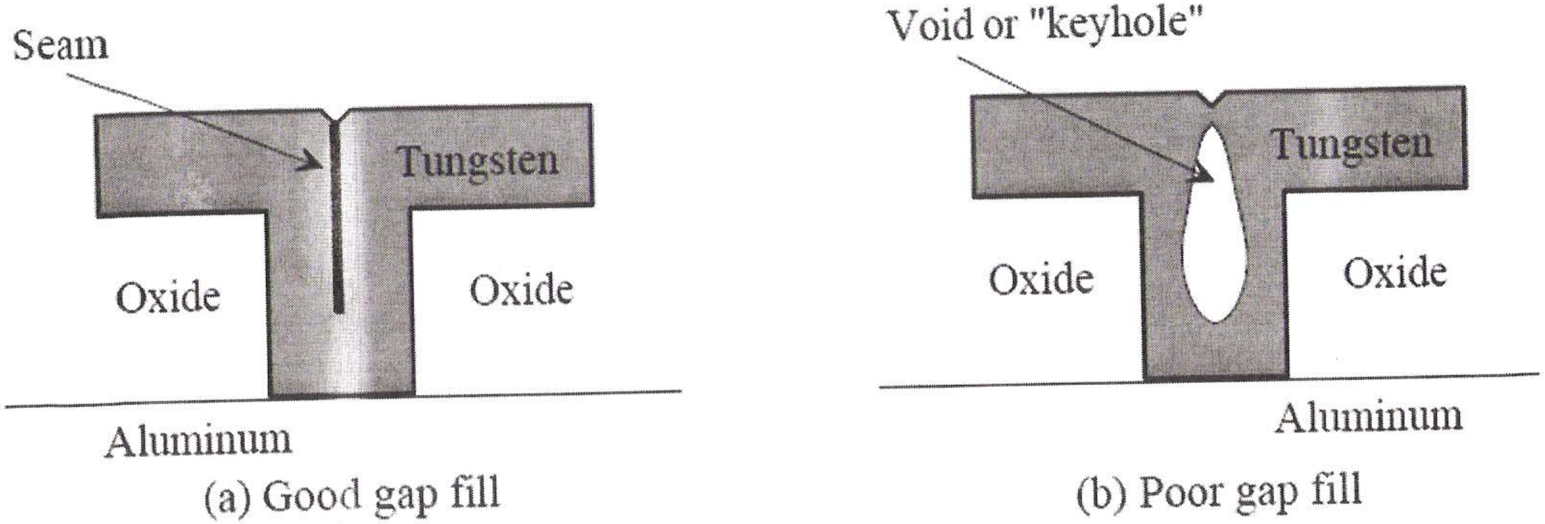

(a) Good gap fill

(b) Poor gap fill

Figure 7.20 Gap-fill profiles (good and bad) of a high aspect ratio opening filled with a deposited film.

Figures from CMOS Circuit Design, Layout, and Simulation, Copyright Wiley-IEEE, CMOSedu.com

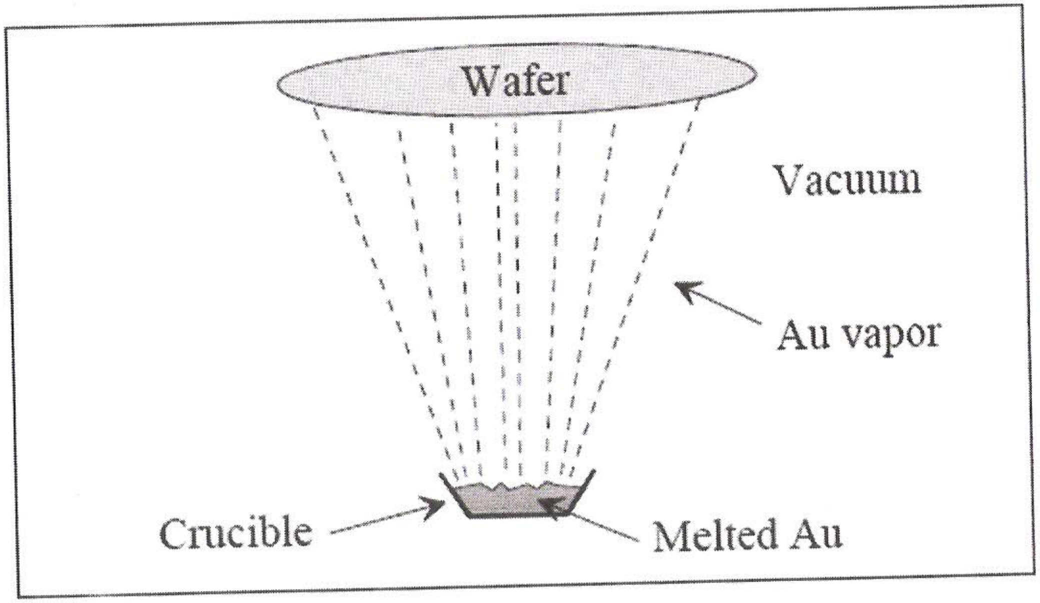

Figure 7.21 Simplified diagram of an evaporation deposition process.

14)

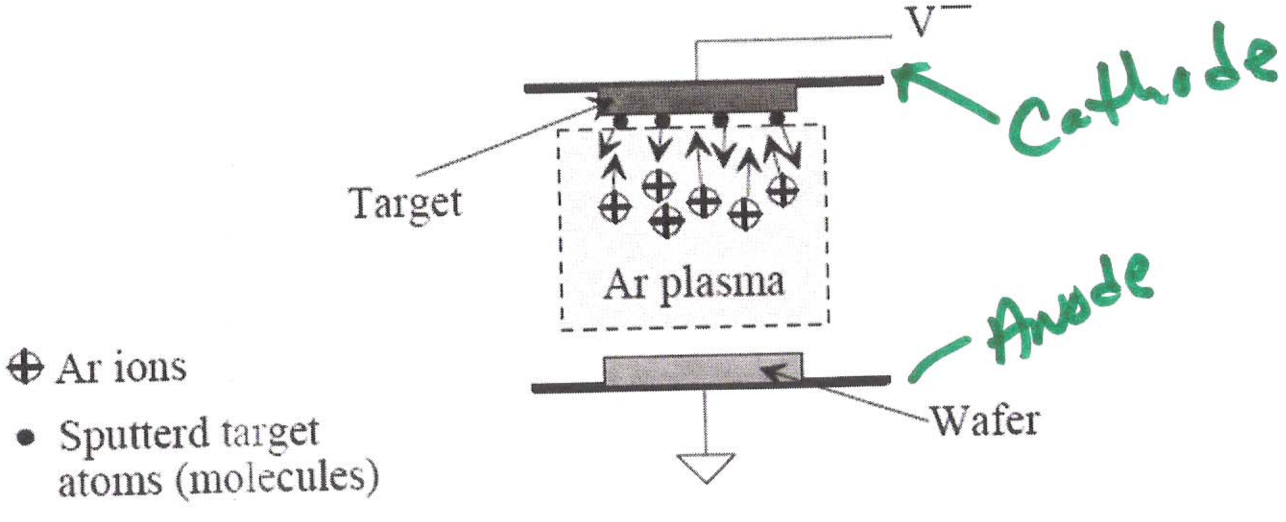

Figure 7.22 Simplified diagram of a sputter deposition process.

15)

Figures from CMOS Circuit Design, Layout, and Simulation, Copyright Wiley-IEEE, CMOSedu.com

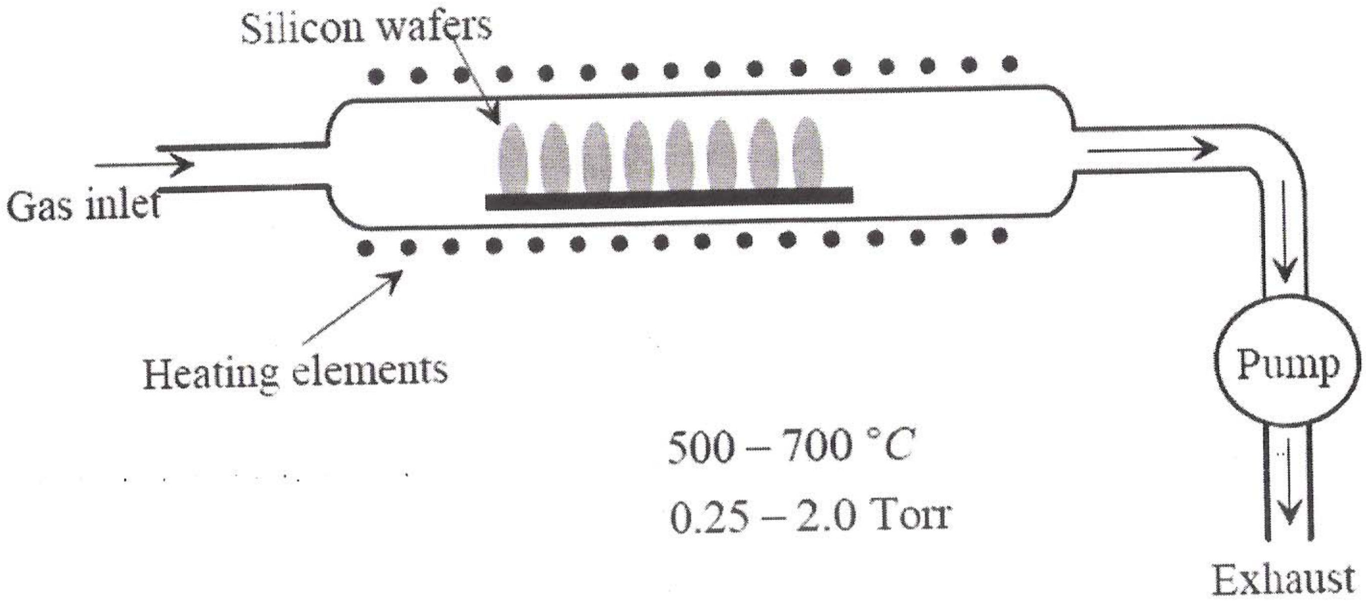

Figure 7.23 Simplified schematic diagram of a LPCVD.

16)

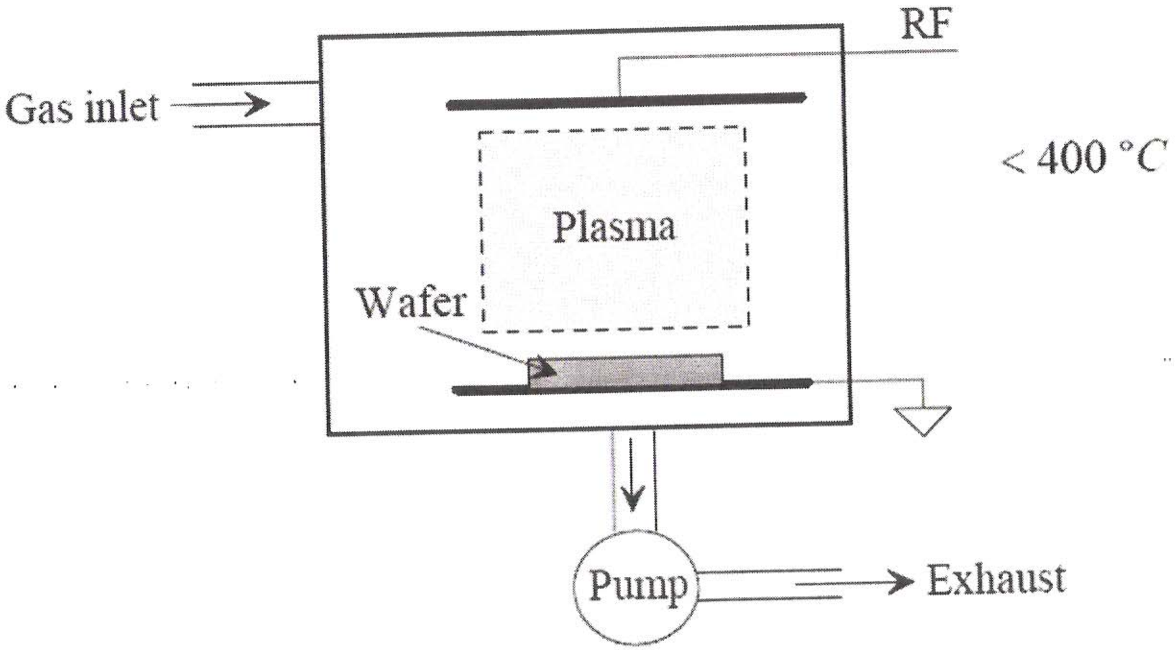

Figure 7.24 Simplified schematic diagram of a PECVD reactor.

17)

Figures from CMOS Circuit Design, Layout, and Simulation, Copyright Wiley-IEEE, CMOSedu.com